Response of a laterally vibrating nanotip to surface forces

Ayhan Yurtsever, Alexander M. Gigler, Eduardo Macias, and Robert W. Stark[a)]
Center for NanoScience (CeNS) and Department of Earth and Environmental Sciences, Ludwig-Maximilians-Universität München, Theresienstrasse 41, 80333 Munich, Germany

(Received 28 August 2007; accepted 29 November 2007; published online 20 December 2007)

The torsional eigenmodes of atomic force microscope (AFM) cantilevers are highly sensitive toward in-plane material properties of the sample. We studied the effect of viscosity and lateral contact stiffness on the detuning, amplitude, and phase response numerically. To verify the theoretical considerations, a torsion mode AFM was operated in frequency modulation. During approach and retract cycles, we observed a negative detuning of the torsional resonant frequency close to the sample surface depending on the tilt angle between the tip and the sample. Thus, the tilt has a significant effect on the imaging process in torsional resonance mode. © *2007 American Institute of Physics*. [DOI: 10.1063/1.2826285]

The tribological characterization of nanomaterials requires friction measurements with very high sensitivity and resolution as can be provided by an atomic force microscope (AFM). To this end, scanning shear force microscopy[1] is a very valuable tool. Several shear force microscopes for measurements with AFM cantilevers but different excitation mechanisms have been reported such as overtone microscopy,[2] combined dynamic mode,[3] ultrasonic torsional contact resonance spectroscopy,[4] or torsional resonance mode using amplitude modulation.[5] The common idea is to measure changes in the response of the torsional cantilever resonance. In torsional resonance mode, a split piezoactuator drives the cantilever at its torsional resonance, typically in the range of 1–2 MHz. This technical approach greatly facilitates shear force microscopy with standard cantilevers. However, coupling of torsional and flexural modes complicates an analytic treatment of torsional cantilever vibrations. Thus, finite element analysis is advantageous for the investigation of the system dynamics. A three dimensional simulation of the torsional resonances clearly showed that flexural bending and torsional oscillations are coupled due to tip-sample interaction.[6]

In the following, we investigate the frequency response of the torsionally vibrating AFM cantilever in order to clarify the role of the tilt between specimen and plane of oscillation. Understanding the influence of the tip-sample interaction on frequency response is essential for a quantitative interpretation of data obtained in torsional resonance mode. The calculations are corroborated by an experiment under ambient conditions, demonstrating the influence of the tilt angle.

For a vertically oscillating tip, the attractive surface potential and viscoelastic sample properties determine the interaction forces. van der Waals forces dominate the interaction in the attractive regime ($\delta < 0$). In the repulsive regime ($\delta \geq 0$), forces can be calculated using a Derjaguin-Muller-Toporov model.[7] Thus, the vertical tip-sample forces are given by

$$F_{\perp}(\delta) = \begin{cases} -HR/[6(\delta - a_0)^2], & \delta < 0 \\ -HR/(6a_0^2) + \frac{4}{3}E^*\sqrt{R}\delta^{3/2}, & \delta \geq 0. \end{cases} \quad (1)$$

Parameter H is the Hamaker constant, R is the tip radius, δ is the indentation depth into the sample, and a_0 is a typical interatomic distance. Distance parameters are defined in Fig. 1(a). The elastic modulus of the tip-sample contact is given by

$$E^* = [(1 - \nu_t^2)/E_t + (1 - \nu_s^2)/E_s]^{-1}, \quad (2)$$

where E_t and E_s are the elastic moduli and ν_t and ν_s are the Poisson ratios of tip and sample, respectively. Linearization

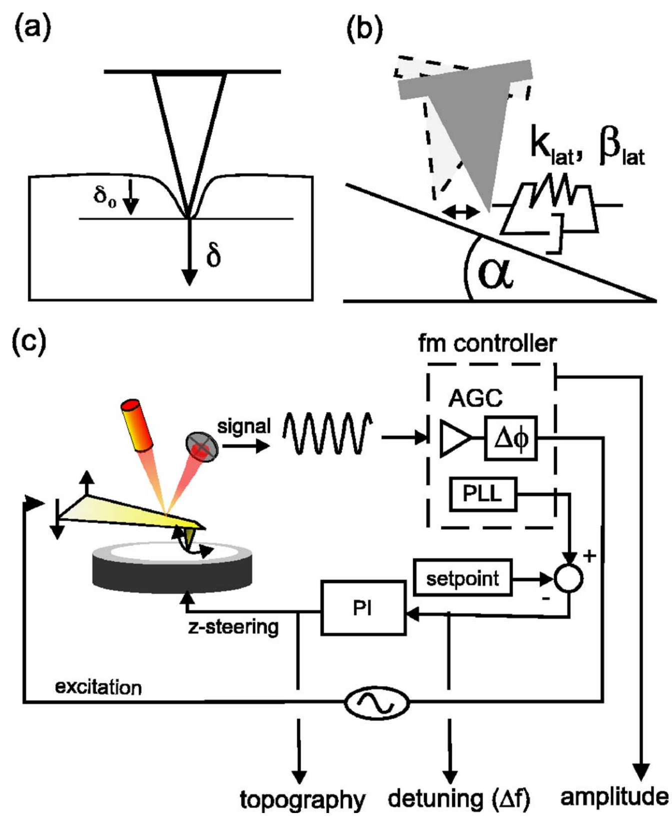

FIG. 1. (Color online) (a) Parameters used to describe the indentation. (b) A laterally vibrating tip interacting with a tilted specimen. (c) Experimental setup of a frequency modulation torsion mode AFM.

[a)]Author to whom correspondence should be addressed. Electronic mail: stark@lrz.uni-muenchen.de. Tel./FAX: +49 89 2180-4329/-4334.

for very small vertical oscillations at a given indentation δ_0 leads to the effective tip-sample stiffness

$$k_\perp = -\frac{\partial}{\partial \delta}F_\perp\bigg|_{\delta=\delta_0} = \begin{cases} -HR/[3(\delta_0 - a_0)^3], & \delta_0 < 0 \\ 2E^*\sqrt{R\delta_0}, & \delta_0 \geqslant 0. \end{cases} \tag{3}$$

For the lateral force, we assume no interaction before contact ($\delta<0$). Within the repulsive regime, we use an elastic interaction as derived from the Hertz model.[8] Thus, we obtain

$$k_{||} = \begin{cases} 0, & \delta_0 < 0 \\ 8G^*\sqrt{R\delta_0}, & \delta_0 \geqslant 0 \end{cases} \tag{4}$$

for the linearized in-plane stiffness. The shear stiffness is $G^* = [(2-\nu_t^2)/G_t + (2-\nu_s^2)/G_s]^{-1}$, where G_t and G_s are the shear moduli and $v_{||}$ denotes an in-plane velocity due to lateral oscillations. We assume that the lateral viscous damping force is dependent on the strain rate and the damping coefficient β in the dissipation process ($F=\beta\dot{\delta}$). In the model, we have neglected friction in the noncontact regime which, for example, can be caused by a liquid neck due to capillary condensation.

If the lateral oscillations occur with respect to a tilted specimen, the in-plane and out-of plane components both contribute to the interaction, as illustrated in Fig. 1(b)

$$k_{\text{lat}} = k_{||}\cos(\alpha) + k_\perp \sin(\alpha),$$

$$k_{\text{norm}} = k_{||}\sin(\alpha) + k_\perp \cos(\alpha). \tag{5}$$

For small angles α, the effective lateral force is given by

$$k_{\text{lat}} = k_{||} + \alpha k_\perp. \tag{6}$$

Notably, an attractive elastic interaction may be introduced to the in-plane component, whereas a dissipative component is added to the normal component due to interfacial friction. Additionally, the elastic contact stiffens. In other words, increasing the tilt angle leads to a transition from a purely frictional (rubbing the surface) to a vibroimpact (tapping and sliding on the surface) regime.

In order to evaluate the response of the cantilever to in-plane surface properties, a finite element (FE) model of a typical cantilever was implemented in COMSOL 3.2/FEMLAB 3.2 (FEMLAB GmbH, Göttingen, Germany), as illustrated in Fig. 2(a). Tetrahedral mesh elements and the following geometry parameters were used: length $L=250$ μm, width $b=40$ μm, thickness $t=3$ μm, Young's modulus $E_t=169$ GPa, Poisson's ratio $\upsilon_t=0.28$, and density $\rho=2330$ kg/m^3. A rectangular cross section of the beam was assumed. The beam ends in a triangle, which resembles the actual shape of such a cantilever. The conical tip was located at $L=220$ μm (cone base diameter $d=12$ μm, height $h=15$ μm, semiangle $\alpha=21.8°$). Mesh refinement was performed in order to check the convergence of the modal solution. Interaction related parameters of the silicon tip and the graphite sample were $H=2.96\times10^{-19}$ J, $G^*=4.2$ GPa, $E^*=10.2$ GPa, $\beta=8\times10^{-7}$ Ns/m, and $a_0=0.38$ nm. The boundary conditions were set according to a clamped end at the cantilever chip. At the tip end, the mechanical coupling is described by a Kelvin-Voigt model assuming a Hookian spring in parallel with a Newtonian dash pot. Since the response to vertical force gradients k_{norm} has been discussed on the basis of numerical and analytic models,[9] we only investigate the effect

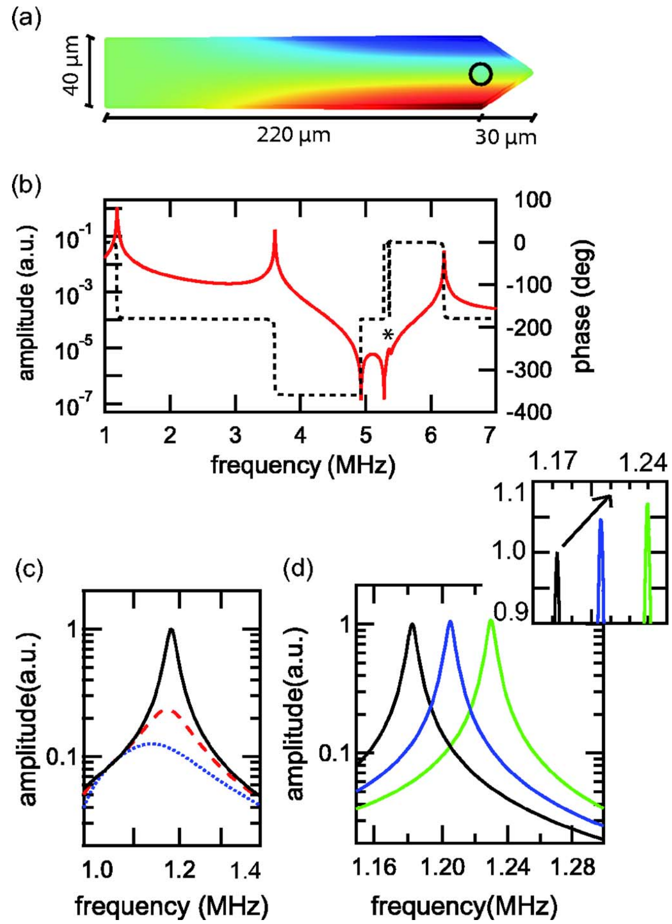

FIG. 2. (Color online) (a) Geometry of the cantilever as used for the finite element analysis. The colors show the shape of the first torsional eigenmode. The circle indicates the base of the conical tip. (b) Torsional frequency response of the freely vibrating cantilever as obtained by finite element analysis. Amplitude response (red, solid) and phase response (black, dash). The asterisk indicates the lateral bending resonance. (c) Amplitude change due to increasing damping: $\beta=8\times10^{-7}$, 4×10^{-6}, and 8×10^{-6} N s/m. (d) Frequency shift caused by elastic interaction (tip-sample stiffness: $k=0$, 13, and 26 N/m). The inset illustrates amplitude increase on a linear scale.

of a lateral stiffness k_{lat} on the characteristics of the torsional oscillator.

The driving force was simulated as a distributed load at the long cantilever edge in the FE model, because, experimentally, a split piezoactuator at the cantilever holder was used to excite the torsional vibration [Fig. 1(c)]. Dynamic frequency response analyses were carried out between 1 and 7 MHz. To account for intrinsic damping, Rayleigh damping was included, assuming a mass-proportional and stiffness-proportional viscous damping.

Figure 2(b) shows the calculated frequency response of the amplitude of a freely oscillating AFM cantilever. For small oscillation amplitudes, the amplitude is proportional to the twist angle. The phase shift remains in the range between 0° and 360°. A lateral bending mode can also be excited (asterisk). Furthermore, we calculated antiresonances at 4.92 and 5.28 MHz. Figure 2(c) shows the amplitude response of the first torsional eigenmode under purely dissipative interaction. The oscillation amplitude decreases with increasing damping parameter β. Figure 2(d) shows the results of the calculation of the amplitude response of the first torsional eigenmode for different contact stiffnesses k_{lat}. With increasing tip-sample stiffness, the resonant frequency increases but the transmission minima stay at the same frequency. Additionally, the torsion angle increase is leading to an increased amplitude measured by the light lever [inset in Fig. 2(d)]. For resonance detuning on the order of 50 kHz, the increase in amplitude is about 0.15%/kHz. This effect is different from a harmonic oscillator where the oscillation amplitude decreases for an increased stiffness. The change in amplitude can be neglected for imaging purposes but becomes relevant in torsional spectroscopy applications, where a detuning on the order of several kilohertz can occur. The physical reason for this amplitude increase is the shift of the torsion axis due to tip-surface coupling. In the case of the free cantilever, the axis of torsion is close to the cantilever main axis. By increasing the tip-sample stiffness to higher values, the tip of the cantilever is increasingly pinned to the sample surface and the torsional axis intersects close to the pinpoint. Thus, torsion angle, as measured by the light lever, can increase (depending of the actual laser beam adjustment). Additionally, tip mass and tip-sample interactions break the twofold rotational symmetry of the cantilever beam. Such a reduced symmetry leads to coupling between closely spaced torsional and bending modes.[10] Thus, geometric effects together with mode coupling can help explain the experimental observation that with increasing load onto the specimen, the power stored in a torsional resonance eigenmode due to thermomechanical excitation apparently decreases while the measured oscillation amplitude increases.[11]

In order to verify the role of sample tilt on the frequency response experimentally, we used a combination of the Dimension 3100 setup with a NanoScope IV controller (Veeco Metrology Inc., Santa Barbara, CA) equipped with torsional resonance mode adapter and probe holder together with a phase-locked-loop Nanosurf Easy PLL (Nanosurf, Liestal, Switzerland/Schaefer Technologie GmbH, Langen, Germany) [Fig. 1(c)]. Silicon cantilevers (ZEIHR, Nanosensors, Neuchâtel, Switzerland) with a typical flexural resonance frequency of 117 kHz and a nominal spring constant of 27 N/m were used for the frequency modulated torsional resonance mode AFM (FM-TR-AFM) measurements. The torsional resonance frequency was 910 kHz. The cantilever was driven using the constant excitation mode where the response time is Q limited. A goniometer (GN05/M, Thorlabs GmbH, Dachau, Germany) was used to change the angle between tip and sample.

Figure 3 shows a typical distance curve of torsional resonant frequency shift versus the z piezotravel on highly oriented pyrolthic graphite. Adjustment of the tilt angle of the sample surface to zero with respect to the cantilever oscillation (i.e., oscillation and the surface are parallel), reveals that long-range interaction forces have little effect on the torsional vibration. However, if the plane of oscillation and the surface are tilted with respect to each other, this angle leads to a mixing of in-plane sample properties with the out-of-plane interaction. In this case, van der Waals forces induce a negative frequency shift of the torsional resonance. This suggests that the negative detuning of the torsional resonance, as also observed by others,[12] is due to a slight tilt between the plane of oscillation and the local specimen surface.

The numerical results together with the experiments help explain the fundamental mechanisms of z feedback in frequency modulated torsional resonance mode AFM (Ref. 13) (FM-TR-AFM). The topography feedback regulates the AFM depending on the detuning of the resonant oscillation.

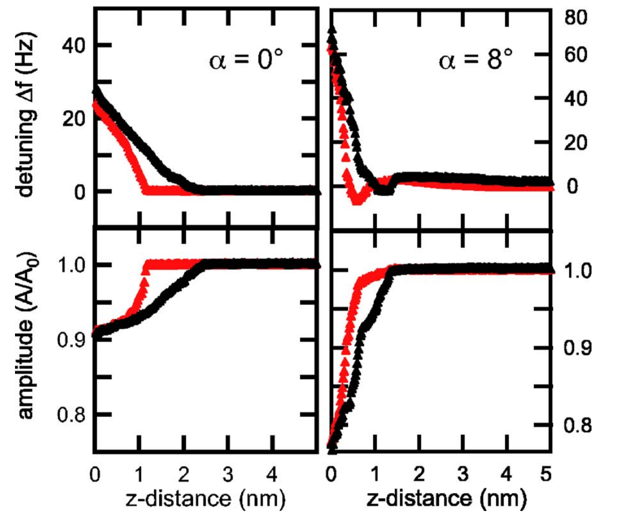

FIG. 3. (Color online) Amplitude and frequency shift measured during an approach (red) and retract (black) cycle on an untilted ($\alpha=0°$) and a tilted ($\alpha=8°$) graphite sample. Note that a negative frequency shift occurs due to attractive forces on the tilted specimen. In the repulsive regime, the detuning response is steeper on the tilted specimen. Free torsional resonant frequency, the quality factor, and the amplitude were 900 kHz, 1300, and 405 mV, respectively.

If tip and sample are properly aligned, positive detuning occurs due to elastic coupling between the tip and sample. This detuning is accompanied by an amplitude reduction due to energy dissipation through the frictional contact. If specimen and oscillator are tilted, additional repulsive as well as attractive forces may occur due to mixing of in-plane and out-of plane properties.

We gratefully acknowledge financial support by the German Federal Ministry of Education and Research, grant Nanofutur 03N8706. A.Y. is supported by the Scholarship of the Elite Network of Bavaria, International Doctorate Program Nano-Bio-Technology (IDK-NBT).

[1]K. Karrai and R. D. Grober, Appl. Phys. Lett. **66**, 1842 (1995); K. Karrai and I. Tiemann, Phys. Rev. B **62**, 13174 (2000); H. Göttlich, R. W. Stark, J. D. Pedarnig, and W. M. Heckl, Rev. Sci. Instrum. **71**, 3104 (2000); A. D. L. Humphris, M. Antognozzi, T. J. McMaster, and M. J. Miles, Langmuir **18**, 1729 (2002).
[2]T. Drobek, R. W. Stark, M. Gräber, and W. M. Heckl, New J. Phys. **1**, 15 (1999).
[3]H. U. Krotil, T. Stifter, and O. Marti, Appl. Phys. Lett. **77**, 3857 (2000).
[4]M. Reinstädtler, U. Rabe, V. Scherer, U. Hartmann, A. Goldade, B. Bhushan, and W. Arnold, Appl. Phys. Lett. **82**, 2604 (2003).
[5]L. Huang and C. M. Su, Ultramicroscopy **100**, 277 (2004); M. Reinstädtler, T. Kasai, U. Rabe, B. Bhushan, and W. Arnold, J. Phys. D **38**, R269 (2005).
[6]Y. X. Song and B. Bhushan, Ultramicroscopy **106**, 847 (2006).
[7]B. V. Derjaguin, V. M. Muller, and Yu. P. Toporov, J. Colloid Interface Sci. **53**, 314 (1975).
[8]R. W. Carpick, D. F. Ogletree, and M. Salmeron, Appl. Phys. Lett. **70**, 1548 (1997).
[9]U. Rabe, K. Janser, and W. Arnold, Rev. Sci. Instrum. **67**, 3281 (1996); R. Vázquez, F. J. Rubio-Sierra, and R. W. Stark, Nanotechnology **18**, 185504 (2007).
[10]M. Reinstädtler, U. Rabe, V. Scherer, J. A. Turner, and W. Arnold, Surf. Sci. **532-535**, 1152 (2003); L. B. Sharos, A. Raman, S. Crittenden, and R. Reifenberger, Appl. Phys. Lett. **84**, 4638 (2004).
[11]S. Maier, Y. Sang, T. Filleter, M. Grant, R. Bennewitz, E. Gnecco, and E. Meyer, Phys. Rev. B **72**, 245418 (2005).
[12]O. Pfeiffer, R. Bennewitz, A. Baratoff, E. Meyer, and P. Grütter, Phys. Rev. B **65**, 161403 (2002); S. Kawai, S. Kitamura, D. Kobayashi, and H. Kawakatsu, Appl. Phys. Lett. **87**, 173105 (2005).
[13]A. Yurtsever, A. M. Gigler, and R. W. Stark, J. Phys.: Conf. Ser. (in press).